31st Annual International Conference of the IEEE EMBS
Minneapolis, Minnesota, USA, September 2-6, 2009

Analysis of Fixed Point FFT for Fourier Domain Optical Coherence Tomography Systems

Murtaza Ali, *Senior Member, IEEE*, Renuka Parlapalli, David P. Magee, *Member, IEEE,* and Udayan Dasgupta, *Member, IEEE*

***Abstract*—Optical coherence tomography (OCT) is a new imaging modality gaining popularity in the medical community. Its application includes ophthalmology, gastroenterology, dermatology etc. As the use of OCT increases, the need for portable, low power devices also increases. Digital signal processors (DSP) are well suited to meet the signal processing requirements of such a system. These processors usually operate on fixed precision. This paper analyzes the issues that a system implementer faces implementing signal processing algorithms on fixed point processor. Specifically, we show the effect of different fixed point precisions in the implementation of FFT on the sensitivity of Fourier domain OCT systems.**

I. Introduction

Optical coherence tomography (OCT) is a non-invasive, non-ionizing technique for imaging tissue structure of highly scattering media with very high resolution of the order of 1-15 μm [1],[2]. It can be used to image turbid tissues such as skin up to depths of 1-2mm. For more transparent tissues like eye, imaging depths of 3-4mm are also feasible. The properties of OCT, make it a highly promising technique for a wide range of clinical applications, both in-vivo and ex-vivo. One of the most successful clinical applications of OCT has been in the field of ophthalmology. OCT can provide images revealing retinal pathology and can be used to diagnose and monitor several retinal diseases like glaucoma and macular edema. OCT has been used in gastroenterology for early diagnosis of tumors, and images delineating substructures of mucosa and sub-mucosa in GI organs have been reported. In addition, dermatological applications of OCT have been demonstrated.

With an increase of applications of OCT systems, commercialization and corresponding miniaturization of such devices become important. With applications in ophthalmology, dermatology and endoscopy, making these systems low power and hand-held are essential for wider use of these devices. Digital Signal Processors have been widely used in various commercial and medical imaging applications to enable low power, battery operated, real time systems. DSPs are well designed to meet the signal processing needs of OCT systems as well [3].

The power/performance efficiency of DSP partly comes from the use of fixed precision mathematical operations. To date, no performance analysis has been reported in literature that considers fixed point operations. Usually, a careful balance between receiver noise and relative intensity noise (RIN) is required in the design of the system, so that the system sensitivity approaches the shot noise limit [4]. Another trade-off is between the sensitivity and the dynamic range of the system [5]. It is, therefore, important to ensure that the following signal processing implementations do not add any additional noise or reduce the system sensitivity or the dynamic range.

Of the two main types of OCT systems (time domain and Fourier domain), the Fourier domain (FD) systems have shown to have superior performance [4],[6]. Irrespective of whether the Fourier domain system is based on swept source laser or with a spectrometer along with a broadband source, one of the essential processing is the Fast Fourier Transform (FFT). The dynamic range of the FFT output varies based on the internal precisions and scaling. In this paper, we focus on the precision issues of FFT implementation and their effects on OCT sensitivity.

This paper is organized as follows. In section II, we provide a short description of OCT systems focusing on the signal processing chain. Section III describes the internal structures of FFT. Finally, in section IV, we present simulated results on the sensitivity of OCT systems of various FFT precisions and scaling strategies.

II. OCT systems: short overview

OCT is based on coherent interference between reference and sample reflections. It uses a standard Michelson Interferometer with a low coherent light source. In the interferometer, the incoming beam is split into the reference path and the sample path which are recombined after reflections from their respective paths to form an interference signal. In FD system, which is of interest for this paper, the spectrum of the interfering signal is captured. This spectrum can either be captured through a spectrometer and CCD combination as shown in Figure 1 or through the use of a swept source where the source frequency is swept over a chosen range and the interference signal is detected through a photo-detector.

M. Ali, D. P. Magee, and U. Dasgupta are with DSP Solutions R&D Center in Texas Instruments, Dallas, TX 75243.

R. Parlapalli is with Medical Imaging DSP group in Texas Instruments, Stafford, TX 77477.

978-1-4244-3296-7/09/$25.00 ©2009 IEEE

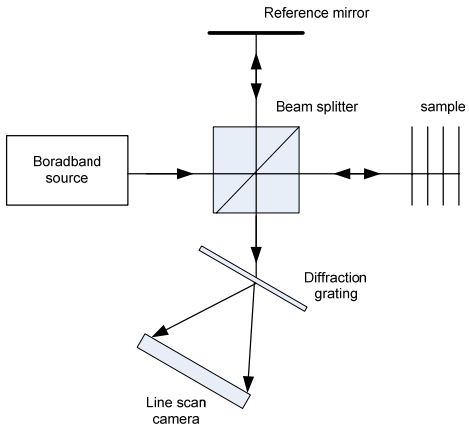

Figure 1: A simplified FD-OCT system diagram

Independent of whether a photo-detector or a CCD camera is used, the detected signal is the average intensity over the frequency region of interest. The detected intensity signal as a function of angular frequency, ω ,can be written as [7]

$$I(\omega,\Delta z)=K_r S(\omega)+K_s S(\omega)\left|H(\omega)\right|^2+ K_i \,\mathrm{Re}\left\{S(\omega)H(\omega)e^{-i\phi(\Delta z)}\right\} \quad (1)$$

Here, K_r, K_s, K_i are constants depending on system design, $S(\omega)$ is the source power spectral density (PSD), $H(\omega)$, the sample frequency response, Δz the path difference between the reference and samples arms, and $\phi(\Delta z)$, the corresponding phase difference.

The sample response function describes the reflections from all the structures in the z direction within the sample and can be written as [7]

$$H(\omega)=\int_{-\infty}^{\infty} r(\omega,z)e^{i2n(\omega,z)\omega z/c}dz \quad (2)$$

Here $r(\omega,z)$ represent the back-scattering coefficients from the sample structures and $n(\omega,z)$ is the refractive index. Note that these terms are frequency and depth dependent.

In FD systems, we can assume $\Delta z=0$. The structure information in the z direction can be recovered by taking the Fourier transform (FT) of the recorded spectrum. i.e.,

$$i(z)=FT\{I(\omega,0)\} \quad (3)$$

The resulting depth resolved structural information is known as 'A' line scan in OCT literature. By moving a mirror assembly (not shown in Figure 1), a set of A line scans can be generated in different directions from which a 2-D or 3-D image can be formed. The detected data is digitized using an analog to digital converter (ADC). The FFT is used to perform the transform in the discrete space.

Depending on the type of systems (whether swept source or spectral radar), the acquired data may not be spaced linearly in the frequency domain which is required to perform the FFT. In systems with CCD detection, the pixel spacing is usually linear in wavelength. Swept source lasers also do not sweep the frequency linearly. Some swept source systems employ a secondary interferometer to extract the clocking information from the source and non-linearly clock the ADC so that the acquired data is linear in frequency [8]. In general, re-sampling is needed to convert input into linearly spaced data. Additional pre-processing includes filtering, averaging, dispersion compensation etc.

Post processing includes determining the magnitude of the FFT which is then compressed to reduce the dynamic range to within the visibility range of the human eye. A generic processing chain for FD-OCT system is shown in Figure 2. Additional post-processing steps like phase extraction may also be needed (e.g., Doppler OCT, polarization sensitive OCT etc.)

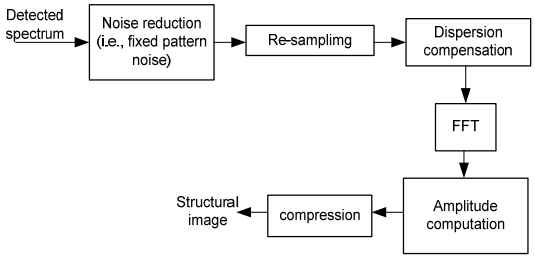

Figure 2: Typical signal processing chain in FD-OCT

III. FFT STRUCTURE

A. Basic FFT Operations

The FFT forms the heart of the computation in the FD OCT systems. FFT is performed on a dataset whose length is a power 2. The operations in FFT can be broken into stages known as radix-4 and radix-2 stages [9]. For data sizes of even powers of 2, only radix-4 operations are needed and for odd powers of 2, one additional stage of radix-2 is needed. The basic operation of radix-4 butterfly can be written as

$$\begin{bmatrix} X_{0,q} \\ X_{1,q} \\ X_{2,q} \\ X_{3,q} \end{bmatrix} = \begin{bmatrix} 1 & 1 & 1 & 1 \\ 1 & -i & -1 & i \\ 1 & -1 & 1 & -1 \\ 1 & i & -1 & -i \end{bmatrix} \begin{bmatrix} W_N^0 x_{0,q} \\ W_N^q x_{1,q} \\ W_N^{2q} x_{2,q} \\ W_N^{3q} x_{3,q} \end{bmatrix} \quad (4)$$

And the basic operations in radix-2 butterfly are as follows

$$\begin{bmatrix} X_{0,q} \\ X_{1,q} \end{bmatrix} = \begin{bmatrix} 1 & 1 \\ 1 & -1 \end{bmatrix} \begin{bmatrix} W_N^0 x_{0,q} \\ W_N^q x_{0,q} \end{bmatrix}. \quad (5)$$

Here, $W_N^k = e^{-i2\pi k/N}$, and N is the size of FFT. The operations are graphically illustrated in Figure 3.

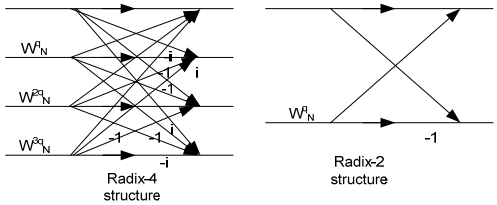

Figure 3: Radix-4 and Radix-2 operations used in FFT

B. Bit Growth

The operations in the butterfly are as follows

- Multiplication by powers of W_N^k commonly referred to as twiddle factors. In fixed point operations, multiplication must be followed by shift to ensure that the most significant bits (MSB) are not lost. This will result in a loss of precision since part of the least significant bits will be lost (LSB)
- Additions and subtractions to produce the outputs of the butterfly stages. In fixed point operations, this stage results in bit growths. To ensure that MSB is not lost, one needs to scale properly. Again doing so results in a loss of precision. In radix-2 operations there will be at best one bit growth per stage and in radix-4 operations, there could be 2 bit growth.

Not all stages in FFT will have a bit growth. So it is not necessary to scale the outputs at every stage. However, this requires analyzing the output of every stage at higher precision before the correct precision of the output can be determined. Other approaches include no scaling with corresponding danger of overflow, scaling at every stage with guarantee of no overflow but reduced precision (reduced dynamic range of output) and selective but pre-determined scaling at every stage. The selection of the scalings at different stages is dependent on signal statistics.

C. FFT bit precisions

In this paper, we present results on two bit precisions. In the first implementation, the twiddle factors are quantized to 16 bits and the internal precision is maintained at 32 bit. We call this 16x32 implementation. With 14 bits of input quantization, this implementation does not require any scaling for the FFT lengths we considered. Only the precision loss due to the loss of LSB in multiplication by twiddle factors and in the quantization of twiddle factors contributes to FFT noise. As we shall show later, this loss is well within acceptable range.

The second implementation uses 16 bits of precision for twiddle factors as above but uses only 16 bits of internal precision. This introduces the additional noise due to bit growth in the additions in each radix stages. However, this 16x16 implementation runs much faster than its 16x32 counterpart [10]. This implementation is very sensitive to how scaling in the intermediate stages are done. Here we show the effect of choosing different scaling strategies on the sensitivity of FD-OCT systems.

IV. RESULTS

A. Simulation Method

In order to simulate the effect of fixed point FFT performance on OCT systems, we have taken the following approaches

- Source is assumed to have a Gaussian distribution.
- Sample consists of a single reflective material. No scattering from surrounding material has been modeled. No dispersive effect is modeled.
- The detected signal is modeled using Equation (2).

The receive signal was discretized linearly in frequency (which will be the case for swept source using non-linear clocking scheme and hence no re-sampler was used). Noise was also added to make the sensitivity around 110 dB. The detected signal was then digitized assuming an ideal 14 bit ADC. The digitized data is finally passed through various FFT implementations and studied for sensitivity.

B. Simulation Parameters

Following is a list of simulation parameters used in our analysis

- Center wavelength of source is 840 nm with Full Width Half Magnitude (FWHM) being 144 nm. The corresponding free space axial resolution is 2.16 μm.
- Number of ADC quantization level is set at 14. We have modeled an ideal ADC. Commercial 14 bit ADC usually provides an effective 12-13 bits. The front end gain was set to ensure that the quantization noise is well below the system noise which was set at 110 dB below unity reflectivity.
- Number of received frequency points was 2048.
- The samples are chosen so that after FFT conversion, the sample distance is half the axial resolution, i.e., 1.08 μm. This corresponds to axial measurement range of 1.1 mm for 2048 point FFT. The corresponding spectral range for collecting the frequency data is 326 nm.
- A balanced detection was assumed so that the DC term due to the reference arm was cancelled.
- A single reflection from the sample with reflectivity set at -40 dB is used to determine sensitivity. The sensitivity can then be calculated by adding 40 dB to the SNR.

C. Results

We plot the magnitude of the FFT output in dB which shows the reflectivity and the noise floor.

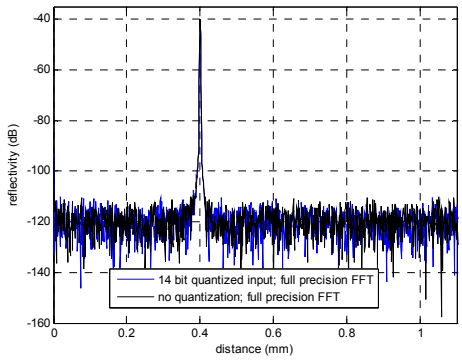

Figure 4: Comparison of performance between full precision input and 14 bit quantization

Figure 4 shows the FFT output for full precision FFT with no input quantization and with 14 bit ADC quantization. There is no visible difference between the two. Thus, the noise floor for our simulated system is not limited by the

ADC. The SNR is seen to be 70 dB making the sensitivity at 110dB. Figure 5 compares the outputs for 14 bit ADC with full precision FFT and with 16x32 fixed precision FFT. There is again no visible difference between the two. Results become interesting when we perform the 16x16 fixed point FFT. Figure 6 shows the output when no scaling is performed to take care of bit growth during the additions in any of the radix stages internally in the FFT. The output shows the effects of overflow which results in false peaks which will be interpreted as reflective objects in OCT systems. On the other hand when scaling is performed at every stage (Figure 7), the system suffers from about 18 dB loss. In this case, the noise characteristics are also different since the noise is primarily determined by the loss of precision in FFT rather than by the input noise. Finally, we choose a strategy where only alternate stages are scaled. The results as seen from Figure 8 show that this case results in no loss of performance compared to full precision FFT providing the best complexity-performance tradeoff.

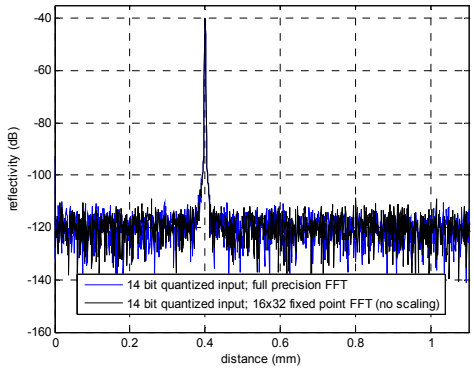

Figure 5: Comparison of performance between full precision FFT and 16x32 fixed point FFT

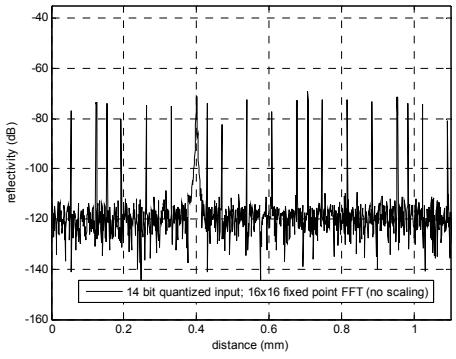

Figure 6: Performance of 16x16 fixed precision FFT with no intermediate scaling

V. CONCLUSION

This paper describes the impact of fixed point FFT implementation on OCT systems sensitivity. For typical OCT configuration, 16 bit input with 32 bit internal precision maintains the same sensitivity as double precision floating point implementation. To use 16 bit internal precision, proper scaling at the intermediate stages of the FFT is needed. This ensures that FFT noise is not the dominating noise. The analysis here is done using a simulated A line scan data with a single reflective sample structure model. Further work will be needed to validate these results with laboratory collected data.

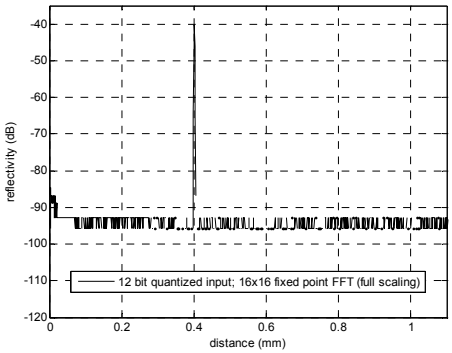

Figure 7: Performance of 16x16 fixed precision FFT with scaling at all intermediate stages

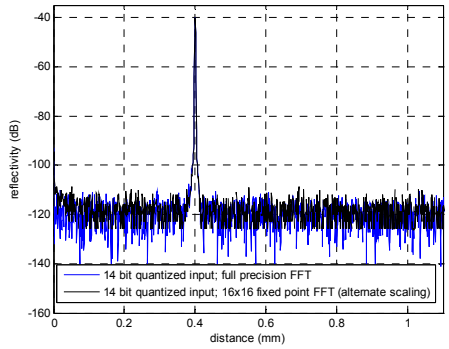

Figure 8: Performance of 16x16 fixed precision FFT with alternate intermediate scaling (compared to full precision FFT)

REFERENCES

[1] A. F. Fercher et al., "Optical Coherence Tomography- Principles and Applications," *Reports on Progress in Physics*, Vol. 66, pp. 239-303, 2003.

[2] J. M. Schmitt, "Optical Coherence Tomography (OCT): A review," *IEEE J. Select. Top. Quant. Electron.*, Vol. 5, No. 4, pp. 1205-1215, 1999.

[3] J. Su et al., "Real-time swept source optical coherence tomography imaging of the human airway using a microelectromechanical system endoscope and digital signal processor, *J. Biomed. Opt.*, Vol. 13(3), 2008.

[4] R. Leitgeb et al., "Performance of Fourier Domain vs. Time Domain Optical Coherence Tomography," *Opt. Express*, Vol. 11(8), pp. 889-894, 2003.

[5] R. A. Leitgeb et al., "Ultrahigh Resolution Fourier Domain Optical Coherence Tomography," *Opt. Express*, Vol. 12(10), pp. 2156-2165, 2004.

[6] M. A. Choma et al., "Sensitivity Advantage of Swept Source and Fourier Domain Optical Coherence Tomography," *Opt. Express*, Vol. 11(18), pp. 2183-2189, 2003.

[7] P. H. Tomlins and R. K. Wang, "Theory, Development and Apllications of Optical Coherence Tomography," *J. of Physics D: Applied Physics*, Vol . 38, pp. 2519-2535, 2005.

[8] D. C. Adler et al., "Three-Dimensional Endomicroscopy Using Optical Coherence Tomography," *Nature Photonics*, Vol. 1, pp. 709-716, 2007, available www.nature.com/naturphotonics.

[9] A. V. Oppenheim and R. W. Schafer, *Discrete-Time Signal Processing*, EngleWood Cliffs, NJ: Prentice-Hall Inc. 1989, ch. 9.

[10] *TMS320C64x+ Little Endian DSP Library Programmer's Reference*, Literature Number: SPRUEB8B, 2008, available http://focus.ti.com/docs/apps/catalog/resources/appnoteabstract.jhtml?abstractName=sprueb8b .